
**AFRL-AFOSR-UK-TR-2024-0012**

# Additive manufacturing with sol-gel

**Gvishi, Raz**
**SOREQ NUCLEAR RESEARCH CENTER (NRC)**
**NAHAL SOREQ**
**YAVNE, , 81800**
**ISR**

**12/13/2023**
**Final Technical Report**



Air Force Research Laboratory
Air Force Office of Scientific Research
European Office of Aerospace Research and Development
Unit 4515 Box 14, APO AE 09421

# REPORT DOCUMENTATION PAGE

**PLEASE DO NOT RETURN YOUR FORM TO THE ABOVE ORGANIZATION.**

| 1. REPORT DATE | 2. REPORT TYPE | 3. DATES COVERED | |
|---|---|---|---|
| 20231213 | Final | START DATE<br>20200901 | END DATE<br>20230831 |

**4. TITLE AND SUBTITLE**
Additive manufacturing with sol-gel

| 5a. CONTRACT NUMBER | 5b. GRANT NUMBER | 5c. PROGRAM ELEMENT NUMBER |
|---|---|---|
| | FA8655-20-1-7050 | |
| **5d. PROJECT NUMBER** | **5e. TASK NUMBER** | **5f. WORK UNIT NUMBER** |
| | | |

**6. AUTHOR(S)**
Raz Gvishi

**7. PERFORMING ORGANIZATION NAME(S) AND ADDRESS(ES)**
SOREQ NUCLEAR RESEARCH CENTER (NRC)
NAHAL SOREQ
YAVNE 81800
ISR

**8. PERFORMING ORGANIZATION REPORT NUMBER**

| 9. SPONSORING/MONITORING AGENCY NAME(S) AND ADDRESS(ES) | 10. SPONSOR/MONITOR'S ACRONYM(S) | 11. SPONSOR/MONITOR'S REPORT NUMBER(S) |
|---|---|---|
| EOARD<br>UNIT 4515<br>APO AE 09421-4515 | AFRL/AFOSR IOE | AFRL-AFOSR-UK-TR-2024-0012 |

**12. DISTRIBUTION/AVAILABILITY STATEMENT**
A Distribution Unlimited: PB Public Release

**13. SUPPLEMENTARY NOTES**

**14. ABSTRACT**
In this project we extended our activity for developing routes for doping functional materials in Sol-Gel matrices. We focused on studying doping of derivatives of an asymmetric Fluorene chromophore, Diphenylamine-Fluorene-Benzothiazole (called AF240). This dye is sensitive to the environment and has significant two forms "green" and "orange", which differ from each other in UV-Vis absorption spectrum and luminescence spectrum, and also in nonlinear optical properties. The "green" form exhibits absorption below 450 nm and luminescence spectrum centered at ~470 nm. This form is stable in non-polar environments resulting in a non-protonated chromophore form. The "orange" form exhibits presence of an additional absorption band centered at 480 nm that extends past 550 nm. The luminescence spectrum of the "orange" form is significantly "red-shifted" and centered at 600 nm. This form is stable in polar environments resulting in a protonated chromophore form. We succeeded to develop a route to dope AF240 derivatives and stabilize them in the two forms. The "orange" form was stabilized in the Sol-Gel matrix when the chromophore was added to the Sol-Gel precursor's solution prior to hydrolysis of the sol. In contrast, the "green" form was stabilized in the Sol-Gel matrix when the chromophore was added to the sol solution after hydrolysis, but before gelation. This research was conducted partially at AFRL and partially at Soreq. The chromophores were supplied by AFRL group. The glassy solid Sol-Gel samples doped with the AF240 chromophore derivatives were prepared at Soreq and preliminary spectral characterization was done. More extensive linear and nonlinear optical spectral characterizations were done at AFRL on the samples sent by Soreq group. In addition, we succeeded to demonstrate fabrication of micro-scale Sol-Gel glassy optical devices using 3D-direct laser writing (DLW) with a 2-photon polymerization (2PP) process. We were able to print 3D structures as micro-scale optical phase elements in various forms - rectangular box, cube, pyramid, and dome. Recently we even demonstrated printing more complex optical devices such as ring-sphere, fiber combiner from one multi-fiber to six single fibers, and mode-sorter on optical fiber tip. We are currently studying the ability to 3D-printing of the nonlinear optical sol-gel filters.

**15. SUBJECT TERMS**

| 16. SECURITY CLASSIFICATION OF: | | | 17. LIMITATION OF ABSTRACT | 18. NUMBER OF PAGES |
|---|---|---|---|---|
| a. REPORT | b. ABSTRACT | c. THIS PAGE | | |
| U | U | U | SAR | 22 |

| 19a. NAME OF RESPONSIBLE PERSON | 19b. PHONE NUMBER *(Include area code)* |
|---|---|
| ATTILA SZEP | 314 235 6044 |

**Standard Form 298** (Rev.5/2020)
Prescribed by ANSI Std. Z39.18

Final Report for EOARD Grant FA8655-20-1-7050

# "Additive manufacturing with Sol-Gel"

November 2023

**By**

**Galit Bar, Ayelet Teitelboim, Moran Ben-Nun and Raz Gvishi,**

*Photonic Materials group, Applied Physics Division, Soreq NRC, Yavne 81800, Israel*

**in collaboration with**

**Ramamurthi Kannan[1,2], Zhenning Yu[1,2], Lauren M. Loftus[1,3], Loon-Seng Tan[1], Tod A. Grusenmeyer[1]**

[1] Air Force Research Laboratory, Materials and Manufacturing Directorate, Wright-Patterson Air Force Base, Dayton, Ohio 45433, USA.

[2]UES, Inc. 4401 Dayton Xenia Rd, Dayton, OH, 45432, USA.

[3]Azimuth Corporation, 2079 Presidential Dr. #200, Fairborn, OH 45342, USA.

**Name of Principal Investigators (PI and Co-PIs):**

- e-mail address : **Raz Gvishi**
- Institution : ***Applied Physics Division, Soreq NRC***
- Mailing Address : ***Soreq NRC, Yavne 81800, Israel***
- Phone : **972-8-9434325**
- Fax : **972-8-9434823**

**AFOSR IPO**: Dr. Attila Szep **AFRL PI**: Dr. Tod A. Grusenmeyer

Period of Performance: 09/1/2020 – 08/31/2023

## Abstract:

The current project's (Grant number: FA8655-20-1-7050) aim was research and development of Sol-Gel materials appropriate for additive manufacturing applications (3D-printing) and nonlinear optical filters. The current project activity is a continuation of a previous project aimed at development of linear and non-linear optical materials based on Sol-Gels doped with functional materials (Grant Number: FA955o-16-i-0201).

In the previous work we developed a set of glassy materials based on the Sol-Gel process with desired properties including UV-curing and controlling the matrix environment. Specifically, a route was developed for doping a two-photon absorber (2PA) platinum complex (E1-BTAF-OH) chromophore, supplied by AFRL, in an aromatic Sol-Gel matrix, allowing stabilizing of the triplet-state form with enhanced nonlinear optical properties. In parallel, a glassy Sol-Gel UV-cured ink was developed and 3D-printing of optical elements were demonstrated.

In the current project we extended our activity for developing routes for doping functional materials in Sol-Gel matrices. We focused on studying doping of derivatives of an asymmetric Fluorene chromophore, Diphenylamine-Fluorene-Benzothiazole (called AF240). This dye is sensitive to the environment and has significant two forms "green" and "orange", which differ from each other in UV-Vis absorption spectrum and luminescence spectrum, and also in nonlinear optical properties. The "green" form exhibits absorption below 450 nm and luminescence spectrum centered at ~470 nm. This form is stable in non-polar environments resulting in a non-protonated chromophore form. The "orange" form exhibits presence of an additional absorption band centered at 480 nm that extends past 550 nm. The luminescence spectrum of the "orange" form is significantly "red-shifted" and centered at 600 nm. This form is stable in polar environments resulting in a protonated chromophore form. We succeeded to develop a route to dope AF240 derivatives and stabilize them in the two forms. The "orange" form was stabilized in the Sol-Gel matrix when the chromophore was added to the Sol-Gel precursor's solution prior to hydrolysis of the sol. In contrast, the "green" form was stabilized in the Sol-Gel matrix when the chromophore was added to the sol solution after hydrolysis, but before gelation. This research was conducted partially at AFRL and partially at Soreq. The chromophores were supplied by AFRL group. The glassy solid Sol-Gel samples doped with the AF240 chromophore derivatives were prepared at Soreq and preliminary spectral characterization was done. More extensive linear and nonlinear optical spectral characterizations were done at AFRL on the samples sent by Soreq group.

In addition, we succeeded to demonstrate fabrication of micro-scale Sol-Gel glassy optical devices using 3D-direct laser writing (DLW) with a 2-photon polymerization (2PP) process. We were able to print 3D structures as micro-scale optical phase elements in various forms - rectangular box, cube, pyramid, and dome. Recently we even demonstrated printing more complex optical devices such as ring-sphere, fiber combiner from one multi-fiber to six single fibers, and mode-sorter on optical fiber tip. We are currently studying the ability to 3D-printing of the nonlinear optical sol-gel filters.

## 1. Introduction:

For several decades there has been an intensive search for organic molecules that will be appropriate for use in nonlinear optics (NLO) for photonics devices. The requirements from such materials are on the one hand, to be with significant effective nonlinear performance and on the other hand to be compatible with the optical and mechanical requirements of optical devices used for optical applications. In order to use organic materials in such applications, significant improvements in nonlinear performance are required. Since the properties of organic molecules can be tailored through molecular engineering, several guidelines and design strategies for optimization of nonlinear performance were suggested [1]. Optimization strategies have included extension of the chain length of the π-conjugated system, as well as creation of a non-uniform electronic cloud. The later can be achieved by altering the strengths of the electron donor (D) and acceptor (A) end groups in both quadrupolar (linear) and multipolar (two dimensional) geometries. Fluorene-based molecules are a well-known promising class of organic dyes which were synthesized following those guidelines, where the fluorene (Fl) moiety is the π center of the 2PA molecule [2-5]. The nonlinear performance of fluorene-based molecules was already studied extensively in liquid solutions [6-8] and as solid polymers [9, 10]. For example, a series of fluorene-based molecules with different geometries such as A-Fl-A, A-π-Fl-π-A, D-π-Fl-π-D, Fl-(π-D)$_3$, A-π-Fl-π-A, Fl-(π-A)$_3$, were studied, where the acceptor moiety used was a benzo-thiazole group and the donor moiety used was a diphenyl-amine group. The obtained 2PA cross-sections, δ, values vary from 1,000 GM up to 10,000 GM depending on the molecule's structure, where the resonant enhancement is more dramatic for asymmetric molecules [6]. In addition, it was found that these molecules exhibit a nonlinear loss which is a combination of a two photon-absorption (2PA) process and an excited state absorption (ESA) process which depends on the laser excitation energy [11]. Other examples of Fluorene-based molecules which were studied as 2PA contained a carbazole group, which is a donor moiety [12], with the geometry D-Fl-D [13]. The issue of enhancement of 2PA cross-sections for asymmetric molecules was studied further for fluorene-based molecules with geometry of D-Fl-A, where D is diphenyl-amine group and A is benzo-thiazole group, chromophore called AF240 [14, 15]. Such asymmetric molecules have indeed enhanced 2PA cross-section values, but on the other hand are less stable and their properties are sensitive to the surrounding environment. An example of the effect of solvent polarity was demonstrated for 6-propionyl-2-dimethylaminolnaphthalene (PRODAN) [16], and for amino styryl pyridinium derivatives (ASPD) [17] and for the D-Fl-A fluorene-based molecules [15]. In all these cases significant "red Stokes shifts" were observed as function of solvent polarity.

Even though studies in different solvent environments been made, devices based on organic molecules in solution are not appropriate for general use in optical applications. Therefore, an intensive effort was made to encapsulate the functional optical molecules in a solid matrix. Sol-gel technology is a well-known method for fabrication of solid glassy materials at low temperature [18] which allows encapsulation of organic molecules [19, 20] and specifically encapsulation of NLO dyes for the use as an optical power limiting (OPL) solid filter [21-24]. The sol-gel process starts from mixing solutions of metal-ortho-organic precursors, commonly Si precursors, which undergo hydrolysis and condensation

to form colloidal sol solutions that further undergo gelation to form a solid matrix, and this is schematically presented in Fig.1. Over the years we demonstrated encapsulation of organic molecules such as laser dyes [25-28] and 2PA chromophores [29-31] in sol-gel materials. The effect of solvent polarity was studied for laser dyes in the sol-gel matrices [32]. In these works, several types of sol-gel matrices were used. In more recent works, glassy encapsulation matrices based on fast sol-gel (FSG) process, were used, as in ref [31]. FSG is a method to prepare crack-free hybrid sol-gel glasses without shrinkage and porosity [33]. The method allows fabrication of a viscous sol–gel resin in a few minutes followed by either thermal or UV-curing requiring several hours or several minutes, respectively [34,35]. The obtained glassy "ink" resin can be used for 3D-printing, optical bonding [36], and even 3D-printing using direct laser writing (DLW) with a 2-photon polymerization (2PP) mechanism [37, 38]. By using a variety of precursors in the FSG process we prepared different types of FSG materials [36]. Recently, we demonstrated the influence of an aromatic sol-gel matrix environment on the spectroscopy of a Pt-complex 2PA chromophore dopant in the FSG matrix [36]. Platinum acetylide chromophores were studied as 2-photon absorbers for the last decade [39–42]. The Platinum acetylide chromophores exhibit in the triplet-state an enhanced 2PA cross-section of the order of >1000 GM [40], due to heavy metal platinum centers which give rise to efficient intersystem crossing to long-lived triplet states [39]. In solution it was found that the triplet state can be stabilized by nonpolar aromatic media such as benzene. By controlling the degree of aromatic environment in the sol-gel matrix we were able to stabilize the triplet-state also in FSG matrix [36].

In the current work we studied the optical properties of asymmetric fluorene-derivative dyes, and their dependence on fabrication formulation for preparing optical solid filters based on hybrid sol-gel glasses. We studied two fabrication formulations of doping the diphenylamine-fluorene-benzothiazole dyes in a hybrid inorganic-organic sol-gel matrix. These dyes have two main forms, "green" and "orange", which differ in other UV-Vis absorption and luminescence spectra, as well as in their nonlinear optical properties [14, 15]. We compared the linear and nonlinear spectroscopic performance of the asymmetric fluorene-derivative dyes in the hybrid inorganic-organic sol-gel matrix to that of the dyes in liquid solution. We were able to stabilize in the hybrid inorganic-organic sol-gel matrix the "orange" form with the enhanced nonlinear properties.

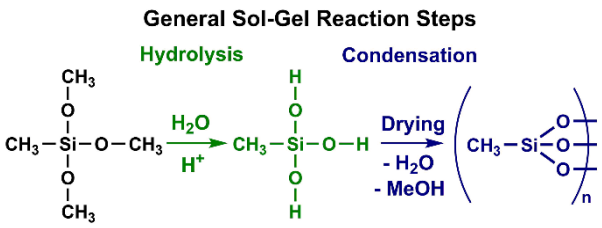


Fig 1: Schematic general sol-gel reaction step with the precursor Methyltrimethoxysilane (MTMS).

In parallel extensive and intensive research was done in the field of 3D-printing of optical devices. We studied the ability to design and print complexed optical devices by direct laser writing [DLW] with 2-photon polymerization (2PP) mechanism using commercial organic photoresist ink printed on crystals

[43] glass slides [44], lenses [45] or directly on an optical fiber tips [46, 47]. Recently we expanded our study and printed optical devices using glassy hybrid inorganic-organic sol-gel ink [37, 38] on glass slide and on an optical fiber tips. Currently we are checking the ability to print the nonlinear optical filters using hybrid inorganic-organic sol-gel ink doped with appropriate 2PA chromophore.

## 2. Experimental section

**Materials and Methods**

The fabrication of the nonlinear optical solid filters consists of two main stages: synthesis of the 2PA chromophores, diphenylamine-fluorene-benzothiazole dyes; and synthesis of the hybrid sol-gel glasses doped with the dye.

**Synthesis of the 2PA chromophores:** Dry DMF, toluene, para-toluene sulfonic acid, potassium carbonate, and ethylene carbonate were purchased from Sigma Aldrich and used as received. N-phenyl-N-(3-hydroxyphenyl)-7-(benzothiazol-2-yl)-9,9-diethylfluoren-2-ylamine and all precursors were prepared as previously reported [48]. Briefly, 8.53 g N-phenyl-N-(3-hydroxyphenyl)-7-(benzothiazol-2-yl)-9,9-diethylfluoren-2-ylamine (15.8 mmol), 2.6 g $K_2CO_3$ (20 mmol), 2.4 g ethylene carbonate (30 mmol), and 75 ml DMF were added to a 250 mL round-bottom flask. The reaction was run at 65° C under $N_2$ for 24 hours followed by the addition of another 1.4 g ethylene carbonate and 1.38 g $K_2CO_3$. The reaction was allowed to run at 65° C under $N_2$ for an additional 24 hours. The reaction was allowed to cool to room temperature and let stand over the weekend. The reaction contents were poured into 500 ml water resulting in the formation of a yellow precipitate. The yellow solid was isolated using medium porosity, fritted glass. Pure Fluorene-$OC_2$ was obtained following a two-step purification process. The crude product was first chromatographed on silica using toluene as the eluent and then recrystallized from isopropanol-methanol to yield the product (7.25 g, 78.8% yield) as yellow crystals. A spectroscopic analysis of the synthesized chromophores was done using $^1H$ and $^{13}C$ NMR. The NMR results are presented in section 3, Fig. 6. The obtained two diphenylamine-fluorene-benzothiazole dyes, AF240, are with geometry of D-π-A, and their molecular structures are shown in Fig. 2, (a) with $OC_2$ tail, (b) with $OC_3$ tail.

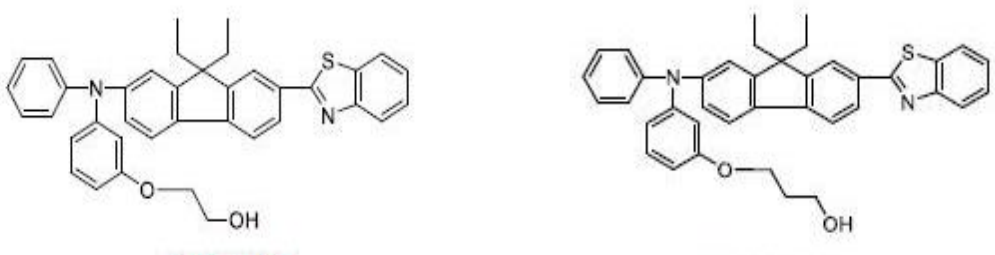


**(a) Fluorene-AF240-$OC_2$** **(b) Fluorene-AF240-$OC_3$**

Figure 2: Diphenylamine-fluorene-benzothiazole dyes, AF240, molecular structures with geometry of D-π-A, (a) with $OC_2$ tail, (b) with $OC_3$ tail.

**Synthesis of the hybrid sol-gel and fabrication of the glasses doped with the dye:** The hybrid inorganic-organic sol-gel was prepared by a fast sol-gel process (FSG) described previously [33]. The precursors used for the preparation of the sol-gel resin are tetramethoxysilane (TMOS), methyltrimethoxysilane (MTMS) and methacryloxypropyl-trimethoxysilane (MATMS). Hydrochloric acid was used as the catalyst and Tetrahydrofuran (THF) as the solvent. All chemicals have a purity of at least 98% and are used as received from Sigma-Aldrich. To produce the catalyst solution, concentrated HCl (37%) is diluted with de-ionized water. Briefly, the synthesis procedure consists of mixing in a reaction bottle TMOS, MTMS and MATMS at a molar ratio of 1:5.6:0.4, respectively, shown schematically in Fig. 3. The catalyst solution of 0.005M HCl was added before the bottle was sealed and placed in a water bath on a heating plate. The mixture was then stirred while heated to 90°C. When the target temperature was reached the pressure in the bottle was released followed by evacuation for 30 seconds. An Alcatel vacuum pump model 2004A with 8 Torr pressure was used to evacuate the volatile products of the hydrolysis-condensation reactions (water and alcohol). An additional minute amount of HCl was added ($7.6 \times 10^{-5}$ mols) before the bottle was sealed again and placed on the hotplate to complete polymerization. 3 to 4 cycles of stirring the mixture at 90°C for 2 minutes and then releasing the pressure and evacuating the excess solvent for 30 seconds followed. By the end of the process a viscous resin was obtained with about 50% of the initial weight due to loss of water and methanol. Finally THF was added for dilution of the viscus resin to allow long shelf life, ratio 1:1 wt. The diluted resin was kept in the sealed bottle at 8°C until the time of use. The organic content of the synthesized FSG is as low as 30% resulting in a more "Silica like" material with high Young's modulus and high transparency at visible and NIR regions [49]. Solidification of the hybrid sol-gel resin was done either by thermal-curing or UV-curing after evaporating the THF on a hotplate at 60°C for several minutes. The thermal-curing was carried out at 60°C in an oven over night, while the UV-curing was carried out with UV-light lamp for few minutes after adding the photoinitiator, Irgacure 184.

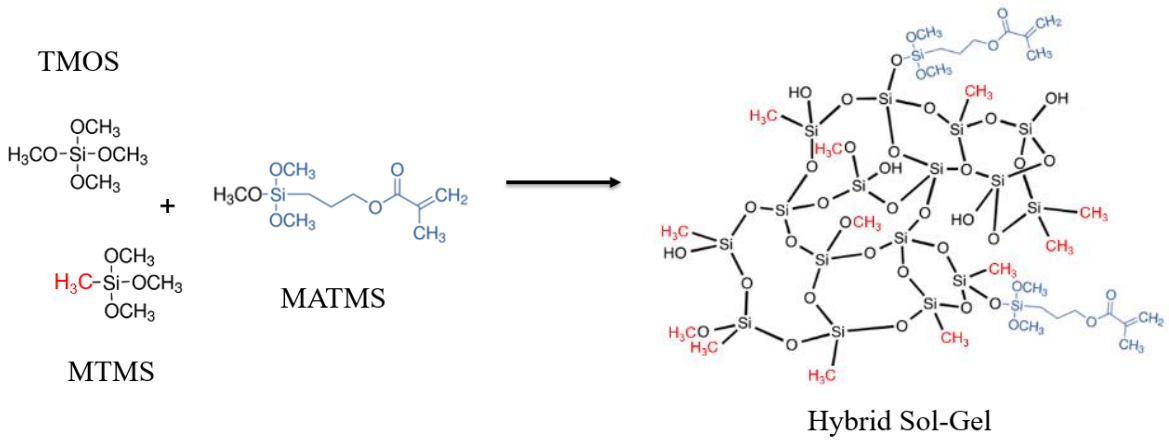


Fig. 3: Schematic drawing of the chemical precursors (TMOS, MTMS and MATMS) and the chemical reactions that follow in the process of making the hybrid FSG

In our sol-gel process the chromophores can be doped into the sol-gel matrix by adding them to the precursor's solution (option “a”) or by adding to the diluted sol (option “b”), shown schematically in Fig. 4. The obtained hybrid sol-gel glass discs were polished to achieve highly transparent flat discs with thickness of 1-2 mm, as shown in Fig. 5. In the case of doping the chromophore diphenylamine-fluorene-benzothiazole, Fluorene-AF240-$OC_2$ dye, both addition options were performed. Option "a" was carried out by adding the dye powder directly to the precursor's solution and dissolving it prior to the hydrolysis. The obtained result was the "orange" form of Fluorene-AF240-$OC_2$ in the hybrid sol-gel glass, seen in Fig. 5a. Option "b" was carried out by dissolving the dye powder in THF solution and adding it to the sol (a colloidal solution) after the hydrolysis. In this case the obtained result was the "green" form of Fluorene-AF240-$OC_2$ in the hybrid sol-gel glass, seen in Fig. 5b.

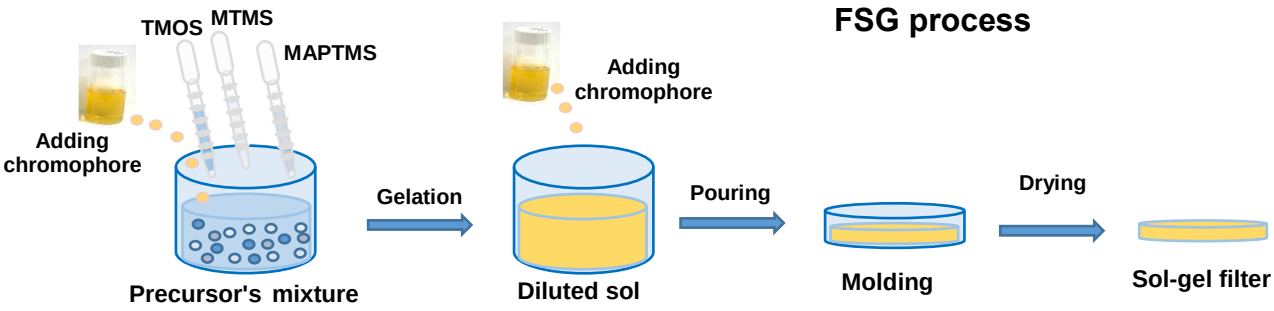


Fig 4: Schematic sol-gel filter fabrication procedure using FSG process. Adding of chromophores to the sol-gel can be done in two options: into the precursor's solution (option “a”) or into the diluted gel solution (option “b”).

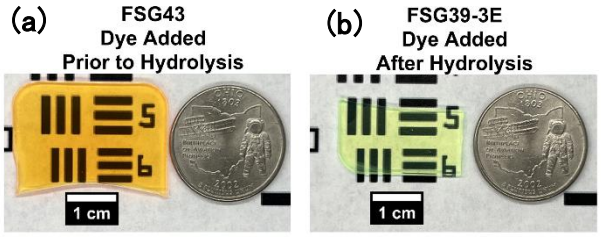


Fig 5: Photos of polished disc of hybrid sol-gel filters doped with diphenylamine-fluorene-benzothiazole, Fluorene-AF240-$OC_2$ dye. (a) Dye added to the precursor solution prior to the hydrolysis, (b) Dye added to the sol solution after the hydrolysis.

### Instrumentation and Measurements

**Linear spectroscopy:** Ground-state UV/vis absorption spectra were measured using either a Jasco V-570 spectrophotometer or a Cary 5000 spectrophotometer. Visible luminescence spectra were obtained using an Edinburgh Instruments FLS980 spectrometer or Ocean Optics HR4000CG fiber spectrometer. In the case of FLS980, the samples were excited using a 450 W xenon lamp attached to a Czerny-Turner monochromator (300 nm focal length, 1800 grooves/mm grating, 1.8 nm/mm linear dispersion) or pulsed LED or laser diode. The emission signal is collected at 90° relative to the excitation source and passed through a Czerny-Turner monochromator (300 nm focal length, 1800 grooves/mm grating, 1.8 nm/mm linear dispersion) prior to being collected with a Hamamatsu R928P side window photomultiplier in a cooled housing (Operating temperature: −20 ℃). In order to correct for the wavelength dependence of the emission light path (i.e. the emission monochromator, PMT detector,

etc.), an emission correction factor was applied. Correction factors were produced by Edinburgh in a two-step process to ensure accuracy. First, the spectra of deuterium and tungsten calibration lamps were acquired. These calibration lamps have a precisely known spectral output traceable to a National Physical Laboratory (NPL) certified spectrum. The emission correction factor is then generated by dividing the lamp spectra measured using the spectrometer by the true spectra of the lamps from NPL. This correction factor was then validated by measuring the reference fluorophores with known emission spectra. The Edinburgh Software converts the slit width in mm to the bandwidth in nm. The bandwidth values reported in the software are given for all experiments.

**Steady-State Luminescence Spectroscopy.** Room temperature steady-state luminescence spectra were collected on fast sol gel (FSG) samples or in toluene solution. FSG39-3E data was collected from 405 – 800 nm after excitation at 400 nm using an excitation bandwidth of 1.0 nm, an emission bandwidth of 0.59 nm, and a 0.500s dwell time. FSG43 data was collected from 490 – 850 nm after excitation at 480 nm using an excitation bandwidth of 1.0 nm, an emission bandwidth of 0.76 nm, and a 0.500s dwell time. AF240 in toluene data was collected from 385 – 700 nm after excitation at 380 nm using an excitation bandwidth of 1.0 nm, an emission bandwidth of 0.30 nm, and a 0.300s dwell time. AF240 in acidic toluene data was collected from 490 – 850 nm after excitation at 480 nm using an excitation bandwidth of 1.0 nm, an emission bandwidth of 0.60 nm, and a 0.200s dwell time. All spectra were collected using a 1 nm step size.

**Time-Resolved Luminescence Spectroscopy.** Room temperature luminescence lifetime measurements were collected on FSG samples or in toluene solution. The luminescence lifetimes were determined using time-correlated single-photon counting. FSG39-3E was excited using a 404 nm pulsed LED source with a pulse duration of 58.8 ps. The luminescence signal was observed at 472 nm and the emission slit width was set so that the emission counts on the detector were 2% of the laser repetition rate. FSG43 was excited using a 506 nm pulsed laser diode source with a pulse duration of 85.0 ps. The luminescence signal was observed at 600 nm and the emission slit width was set so that the emission counts on the detector were 2% of the laser repetition rate. AF240 in toluene was excited using a 404 nm pulsed LED source with a pulse duration of 58.8 ps. The luminescence signal was observed at 475 nm and the emission slit width was set so that the emission counts on the detector were 2% of the laser repetition rate. AF240 in acidic toluene was excited using a 506 nm pulsed laser diode source with a pulse duration of 85.0 ps. The luminescence signal was observed at 600 nm and the emission slit width was set so that the emission counts on the detector were 2% of the laser repetition rate.

**NMR**

Analysis of the synthesized chromophores was done using $^{1}H$ and $^{13}C$ NMR. The NMR experiments were performed on a Bruker NMR spectrometer, with Ascend 400 magnet and AVANCE NEO Console, operating at 400.23 MHz for proton spectrum acquisition and 100.63 MHz for carbon spectrum acquisition. The sample was dissolved in 99.8% pure deuterated chloroform with 0.1% (v/v) tetramethylsilane (TMS) added as the internal standard. The NMR results are presented in section 3, Fig. 6.

**Photopolymerization and printing procedure**

A commercial DLW system (Nanoscribe© Photonic Professional GT) is utilized to perform the printing and polymerization processes. This system comprises of a pulsed erbium-doped femtosecond fiber laser that emits 100 fs pulses at 780 nm with an 80 MHz repetition rate, 150 mW maximum average power, and 25 kW peak power. The beam is focused with a ×63 microscope objective (alternatively, ×25 objective), resulting in a voxel diameter of 0.2 μm with aspect ratio of 3.5 for ×63 (0.6 μm with aspect ratio of 6 for ×25). A drop of the ink is deposited on a glass slide, while a drop of oil is deposited on the opposite side (objective side) of the slide for oil-immersion configuration. The slide is then placed in the 3D printer, and the programmed voxels are polymerized according to a STL file defining the desired three-dimensional structures. After the exposure, the material is developed by immersing the printed elements in acetone for 2 minutes to remove unexposed material, followed by soaking in isopropanol and finally drying in nitrogen. To complete the polymerization and evaporate any remaining THF, the sample was heated overnight under 50° C at ambient pressure.

## 3. Results and Discussion

Two chromophores of diphenylamine-fluorene-benzothiazole dyes were synthesized, Fluorene-$OC_2$ and Fluorene-$OC_3$. The synthesis procedure was detailed in section 2, Fig. 2. Confirmation of the dyes' structures was done using $^1H$ and $^{13}C$ NMR on the obtained yellow crystals of the dyes. The NMR experiments results for N-phenyl-N-(3-phenoxyethanol)-7-(benzothiazol-2-yl)-9,9-diethylfluoren-2-ylamine (Fluorene-$OC_2$) are presented in Fig. 6. $^1H$ chemical shifts are reported in parts per million ($\delta$) with integration and multiplicity (s = singlet, d = doublet, t = triplet, q = quartet, dd = doublet of doublets, dt = doublet of triplets, td = triplet of doublets, ddd = doublet of doublet of doublets, and m = multiples), referenced to TMS as 0 ppm). $^{13}C$ chemical shifts are reported in parts per million referenced to TMS as 0 ppm. The $^1H$ NMR results are presented in Fig 6a and the peaks values are listed: (400 MHz, $CDCl_3$) δ= 8.08(m, 2H), 8.01 (dd, *J*=1.5, 8.0 Hz, 1H), 7.89(d, *J*=8.0 Hz, 1H), 7.69 (d *J*=7.9 Hz, 1H), 7.61 (d, *J*= 8.2 Hz, 1H), 7.48 (t, *J*=7.7 Hz, 1H), 7.37 (t, *J*=7.6 Hz, 1H), 7.27(t, *J*=7.6 Hz, 2H), 7.17 (m, 4H), 7.05(m, 2H), 6.72(m, 2H), 6.58 (dd, *J*=2.4, 8.3 Hz, 1H), 3.98(t, *J*=4.1 Hz, 2H), 3.89(t, *J*=4.6 Hz, 2H), 2.09 (m, 3H), 1.94 (dq, =7.3,14.3 Hz, 2H), 0.38(t, =7.3 Hz, 6H). The $^{13}C$ NMR NMR results are presented in Fig 6b and the peaks values are listed: (101 MHz, $CDCl_3$) δ= 168.83, 159.50, 154.22, 152.08, 150.70, 149.17, 147.90, 147.63, 144.43, 135.56, 134.91, 131.53, 129.92, 129.29, 127.28, 126.27, 124.96, 124.50, 123.59, 123.11, 122.93, 121.53, 121.45, 121.03, 119.41, 119.09, 116.67, 110.06, 108.74, 69.07, 61.38, 6.42, 32.62, 8.61. HRMS (ESI-MS, $[M+H]^+$) m/z calcd for $MH^+$.

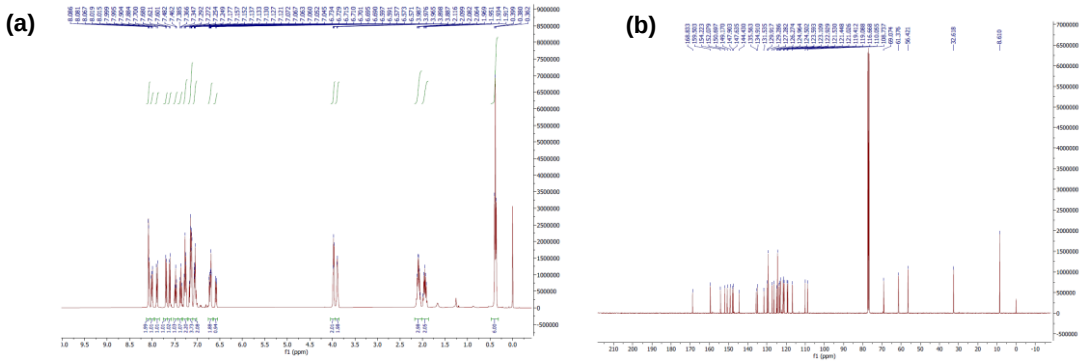


Figure 6: NMR analysis of Fluorene-$OC_2$ collected in d-chloroform; (a) $^1H$ NMR, (b) $^{13}C$ NMR.

Fast sol gel (FSG) glasses containing the chromophore, N-phenyl-N-(3-phenoxyethanol)-7-(benzothiazol-2-yl)-9,9-diethylfluoren-2-ylamine (Fluorene-$OC_2$), were prepared with concentration of ~0.4 mg/ml. Fluorene-$OC_2$ was specifically selected for this study due to the presence of the phenoxyethanol substituent. This allows for crosslinking of the chromophore into the sol gel glass, increasing the chromophore loading and prohibiting aggregation. Doping of the dye into the FSG matrix samples was done using two different formulations: adding the dye to the precursor's solution (option "a") or by adding to the diluted gel solution (option "b"), as was explained in section 2, Fig. 4. The color of the resultant FSG glass was highly dependent on when the Fluorene-$OC_2$ chromophore was added to the formulation. "Orange" colored FSG glasses were obtained when Fluorene-$OC_2$ was added prior to hydrolysis and "green" colored FSG glasses were obtained with Fluorene-$OC_2$ was added after hydrolysis. Optical characterization of the glasses was performed to examine differences in the

photophysical behavior of the materials and to help explain the observed difference in color. Specifically we studied the spectroscopy of two samples; sample FSG43, which was prepared by doping the dye with option "a" – before hydrolysis, resulting in "orange" dye form (Fig. 7a) and sample FSG39-3, which was prepared by doping the dye with option "b" – after hydrolysis, resulting in "green" dye form (Fig. 7b). After polishing, the thickness of sample FSG43 was 1.9 mm and that of sample FSG39-3 was 1.5 mm. Fig 7c presents the UV-NIR spectrum of the two dye-doped sol-gel samples. Both samples exhibit absorption peaks in the range 1100-2500 nm due to the sol-gel matrix as was already reported [49]. In the range 600-1100 nm both samples are fully transparent. In the range 350-450 nm there is in both samples major absorption peak of the dye due to $\pi \rightarrow \pi^*$ transition. While for sample FSG43 the "orange" dye form there is additional absorption peak at ~500 nm, can be seen in Fig. 7c. The visible luminescence spectra of both sol-gel glasses, FSG43 and FSG39, excited at 405 nm, are shown in Fig. 7d. The "green" sample (FSG39) exhibits emission peaking at ~475nm with small red Stokes-shifts due to strong reabsorption effect. The "orange" sample (FSG43) exhibits two emission peaks at ~475nm and at ~625nm with a large red Stokes-shifts.

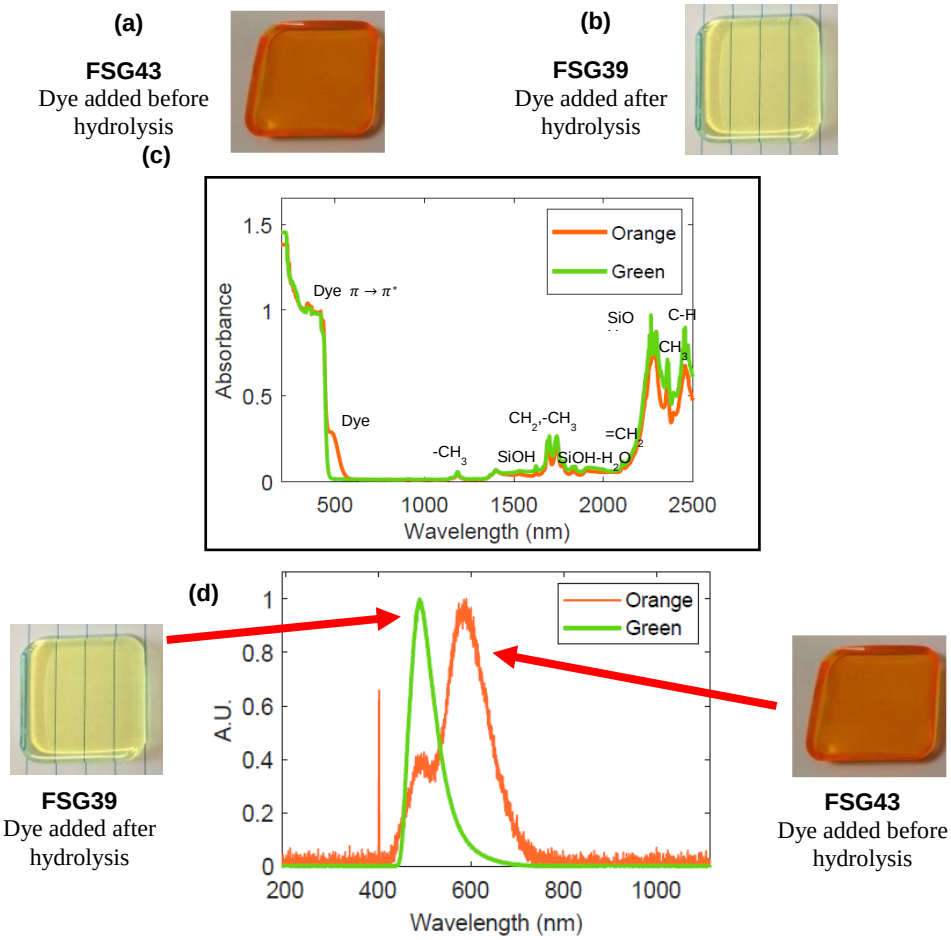


Figure 7: Photos and absorption spectra of hybrid sol-gel doped with Fluorene-AF240-$OC_2$ dye. (a) Photo of sol-gel glass with dye added to the precursor solution prior to the hydrolysis – "orange" form, sample FSG43. (b) Photo of sol-gel glass with dye added to the sol solution after the hydrolysis – "green" form, Sample SFG39. (c) UV-NIR absorption spectra of both sol-gel glasses, FSG43 and FSG39. (d) Visible luminescence spectra of both sol-gel glasses, FSG43 and FSG39 excited at 405 nm.

We conducted additional extended and accurate spectroscopic measurements in order to study Fluorene-$OC_2$ chromophore doped in sol-gel glasses. UV-Vis absorption as well as steady-state and time-resolved luminescence experiments were performed on "green" (FSG39-3E) and "orange" (FSG43) FSG glass samples. Absorbance and steady-state and time-resolved luminescence data for each FSG sample are shown in Fig. 8. Each of the samples possesses unique optical properties. The green color of FSG39-3E is the consequence of strong absorption from 350 nm – 450 nm. The absorbance of the sample plateaus across this wavelength region. This is due to low light transmission of these wavelengths due to the high molar absorptivity of diphenylamine-fluorene-benzothiazole dyes and thickness of the FSG samples (thickness 1.5 mm and 1.9 mm, respectively). The orange color of the FSG43 glass results from the presence of an absorption band centered at 480 nm that extends past 550 nm. The steady-state luminescence spectrum of FSG39-3E is featureless and centered at 471 nm while the steady-state luminescence spectrum of FSG43 is featureless and centered at 600 nm. The steady-state luminescence spectrum of FSG43 (full width at half maximum (fwhm = 123 nm), is significantly broader than the steady-state luminescence spectrum of FSG39-3E (fwhm = 79 nm). The luminescence lifetime of FSG39-3E was determined to be 3.6 ns. This is nearly a factor of two shorter than the luminescence lifetime of FSG43 which was determined to be 6.2 ns. These results are consistent with chromophores that possess different ground- and excited states. The chromophore present in FSG43 possesses either a HOMO or LUMO that is stabilized relative to the HOMO or LUMO of the chromophore present in FSG39-3E due to the presence of the low energy absorption transition in FSG43. The chromophore present in FSG43 also possesses a unique excited-state relative to the chromophore present in FSG39-3E due to the broader luminescence spectrum and longer lifetime of the chromophore present in FSG43. In order to clarify the structural difference which accounts for these unique optical properties we conduct additional study of the optical properties of the chromophores in solutions.

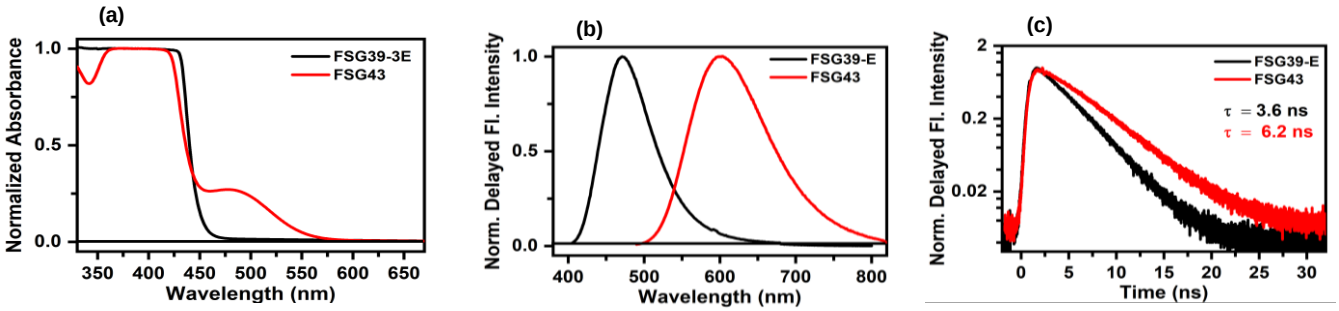


**Figure 8.** (a) Ground-state absorption spectra of FSG39-3E (black) and FSG43 (red) glasses, (b) steady-state luminescence spectra obtained from FSG39-3E (black) and FSG43 (red) glasses, and (c) time-resolved luminescence decays obtained from FSG39-3E (black) and FSG43 (red) glasses.

Fluorene-$OC_2$ is an asymmetric fluorene-based molecule with geometry of D-Fl-A, and due to the asymmetric structure it is highly sensitive to the chemical environment it experiences by the surrounding solid matrix or solution. The sensitivity is related to the polarity of the environment as was observed previously in solution for AF240 [15] and for other dyes in solution and sol-gel glasses [16, 17, 32]. In addition, during the hydrolysis stage in the synthesis of the sol-gel glass the chromophore experienced an acidic environment. This led to the hypothesis that the orange color of FSG43 is the result of

protonation of the nitrogen in the benzothiazole subunit of Fluorene-$OC_2$. Therefore, in order to understand the color dependence, due to the different doping formulations in sol-gel glasses, we studyed the spectroscopic properties of the chromophore in two solvents. A series of control experiments were performed in solution using the parent dye, N-diphenyl-7-(benzothiazol-2-yl)-9,9-diethylfluoren-2-ylamine (AF240). One set of experiments was performed in toluene, which is an aromatic non-polar solvent. A second set of experiments was performed in toluene containing the organic acid, para-toluene sulfonic acid (pTsOH), which is a polar solvent. Absorbance and steady-state and time-resolved luminescence data of AF240 in toluene and AF240 in acidic toluene are shown in Fig. 9. The results of all three solution control experiments mirror the results obtained in FSG glass. The absorption spectra of AF240 in toluene and acidic toluene were collected on dilute solutions (< 1 μmolar) allowing for the resolution of absorption features in solution. The ground-state absorption spectrum of AF240 in toluene shows a structured absorption band with a maximum at 390 nm that tails to 450 nm. The ground-state absorption spectrum of AF240 in acidic toluene features an additional absorption band centered at 480 nm that tails past 530 nm. The steady-state luminescence spectrum of AF240 in toluene is centered at 450 nm, while the steady-state luminescence spectrum of AF240 in acidic toluene is featureless and centered at 600 nm. The steady-state luminescence spectrum of AF240 in acidic toluene (fwhm) = 105 nm is significantly broader than the steady-state luminescence spectrum of AF240 in toluene (fwhm = 60 nm). The luminescence lifetime of AF240 in toluene was determined to be 1.5 ns. This is a factor of two shorter than the luminescence lifetime of AF240 in acidic toluene which was determined to be 3.2 ns. A protonation of the nitrogen in the benzothiazole subunit of Fluorene-$OC_2$ and AF240 was suggested to occur in the acidic toluene solution. A depiction of the protonated and non-protonated forms of Fluorene-$OC_2$ are shown in Fig. 10. Protonation of the nitrogen in the benzothiazole subunit of Fluorene-$OC_2$ and AF240 will lower the reduction potential of the chromophore. This will result in a stabilization of the LUMO in Fluorene-$OC_2$-$H^+$ and AF240–$H^+$ relative to Fluorene-$OC_2$ and AF240, accounting for the low energy absorption transition in FSG43 solid sample and AF240 in acidic toluene. The stabilization of the LUMO and formal positive charge on Fluorene-$OC_2$-$H^+$ and AF240-$H^+$ also enhances the probability of charge transfer character in the excited-state of Fluorene-$OC_2$-$H^+$ and AF240–$H^+$ relative to Fluorene-$OC_2$ and AF240. Enhanced charge transfer character is a feasible explanation for the increased fwhm of the steady-state luminescence spectra and longer luminescence lifetimes of FSG43 and AF240 in acidic toluene relative to FSG39-3E and AF240 in toluene. The observation of longer luminescence lifetimes in the FSG glass samples (Fig. 8c) relative to the solution samples (Fig. 9c) is the only discrepancy between these datasets. Incorporation of the chromophores in a solid matrix likely results in diminished non-radiative decay in the excited-states of Fluorene-$OC_2$-$H^+$ and Fluorene-$OC_2$ relative to AF240–$H^+$ and AF240 in solution. This provides a likely explanation for the enhanced lifetime values in the solid samples.

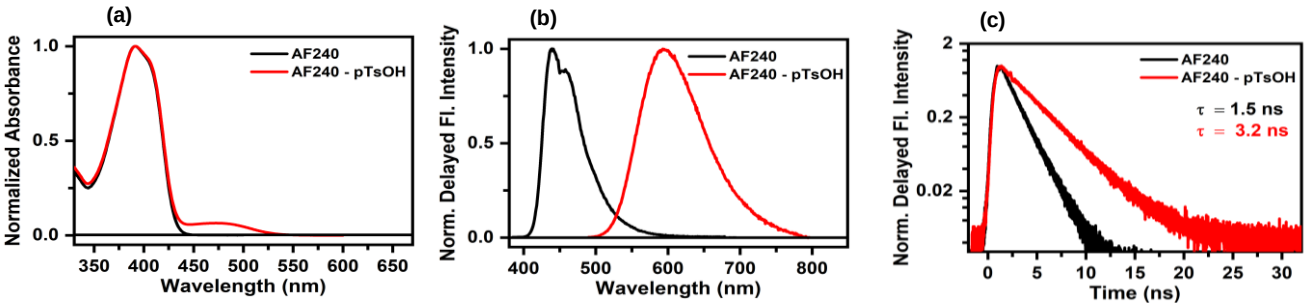


Figure 9: (a) Ground-state absorption spectra of AF240 in toluene (black) and AF240 in acidic toluene (red), (b) steady-state luminescence spectra obtained from AF240 in toluene (black) and AF240 in acidic toluene (red), and (c) time-resolved luminescence decays obtained from AF240 in toluene (black) and AF240 in acidic toluene (red).

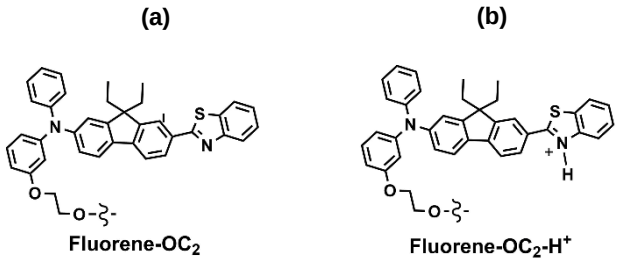


Figure 10: Chemical structures of the Fluorene-$OC_2$ chromophore (a) the initial structure, Fluorene-$OC_2$ (b) the protonated structured, Fluorene-$OC_2$-$H^+$.

An additional way to explain the difference in optical properties between the two forms, green and orange, of Fluorene-$OC_2$ is through the effect of solvent polarity on Stokes shifts, a solvatochromic effect, which was discussed in the introduction. As already mentioned the solvatochromic effect of AF240 in solutions was already studied for solvents [15], and figure 6 in ref [15] presents the Lippert plot (Stokes shifts ($\Delta\nu$) versus solvent polarity parameter ($\Delta f$)) and obtained a strong dependences. Our current results of AF240 Stokes shifts in toluene and acidic toluene were fitted to the previous plot, $\Delta\nu$ =3400 $cm^{-1}$ & $\Delta f$=0.0135 in toluene and $\Delta\nu$ =8970 $cm^{-1}$ & $\Delta f$=? in acidic toluene. However, the difference in Stokes shifts between the two forms (green and orange) in the sol-gel glasses cannot be explained by the macroscopic solvent polarity of the two sol-gel glasses since in both cases the sol-gel matrix exhibits the same macroscopic optical properties, such as refractive index of about 1.44. It was already demonstrated that by using solvatochromic dyes, such as asymmetric fluorescent molecules, doped in sol-gel matrices, the microenvironment of the sol-gel can be probed [16]. In our case we can define two distinguishable microenvironment segments. The first segment is obtained when the Fluorene-$OC_2$ dye is doped by option "a", added to the precursors solution before hydrolysis. In this case, the solvatochromic dye exhibits a polar environment reached with acidic, therefore we can assume the dye is caged inside the sol-gel sols (seen in Fig. 11a). The second segment is obtained when the Fluorene-$OC_2$ dye is doped by option "b", added to the sol solution after hydrolysis. In this case, the solvatochromic dye exhibits a more non-polar environment, therefore we can assume the dye is caged between the hybrid sol-gel chains and attached to the methyl tails (seen in Fig. 11b).

We have studied also the energy level structure of the orange sample, FSG43, using femtosecond transition absorption (fsTA) with pump excitation at 515nm at the range of 1ps to 6.4ns. The results (shown in Fig. 12a) present that at ~540nm (ground-state absorption) the absorption change decreases with excitation time, at ~900nm (excited-state absorption) the absorption change also decreases with excitation time with emission lifetime of 2.1ns (Fig 12b), while at ~610nm the bleach peak population

depletes with excitation time which might indicates an intramolecular charge-transfer (ICT) with time. These results are compatible to the suggested energy level diagram presented in ref [15], fig 11, where for AF240 in a polar solvent several ICT transitions are induced which allow several excited-state absorption (ESA) transitions. The existence of ESA transitions suggest that the orange form of Fluorene-$OC_2$ dye is a good candidate for nonlinear optical absorption performance.

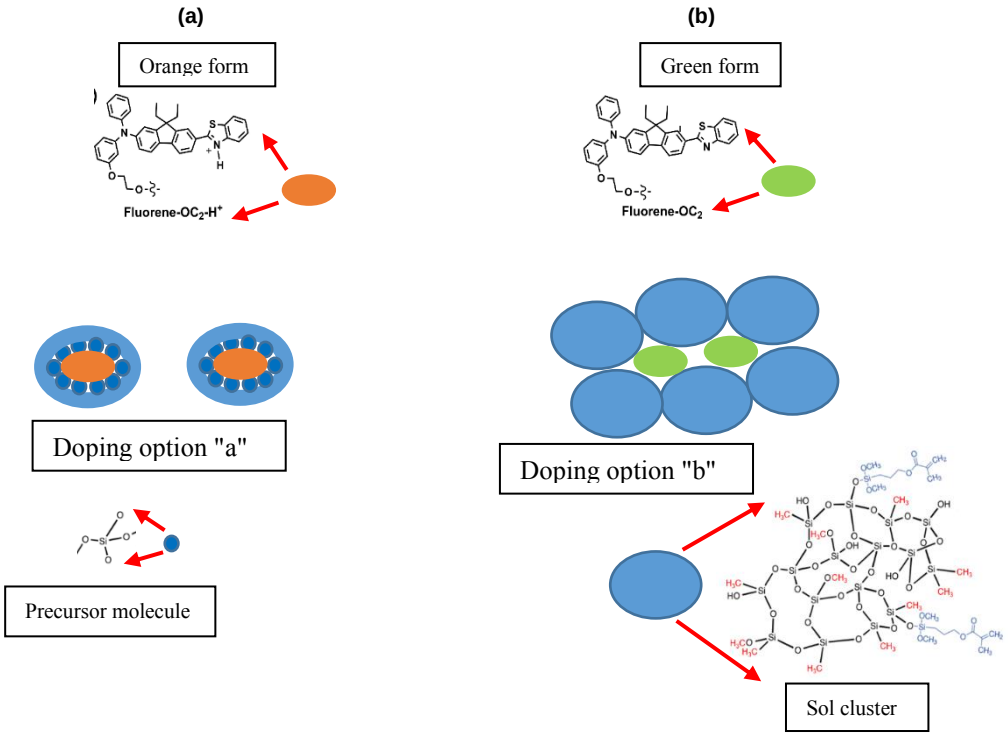


Figure 11: Scheme of doping Fluorene-$OC_2$ in hybrid sol-gel matrix. (a) Doping option "a" – adding the dye to the precursor's solution, before hydrolysis – caging inside the sols. (b) Doping option "b" – adding the dye to the sol solution, after hydrolysis – caging between the particles.

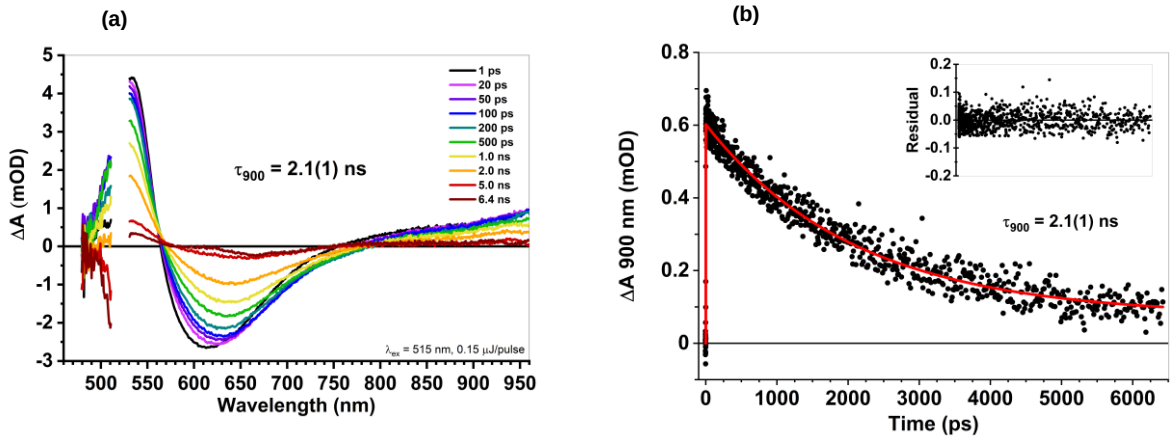


Figure 12: Femtosecond transition absorption (fsTA) spectra of the orange form of Fluorene-$OC_2$ in hybrid sol-gel matrix, sample FSG43. (a) fsTA curves with pump excitation at 515 nm taken in the range of 1ps to 6.4 ns. (b) fsTA lifetime monitoring at 900 nm.

An additional activity which has been done is 3D-printing of micro-scale optical devices. 3D-direct laser writing (DLW) by 2-photon polymerization (2PP) process was used to print the micro-scale optical devices using a commercial DLW system (Nanoscribe, Germany). The material which was used as the photoresist ink for the 3D-printing was an advanced hybrid organic-inorganic material made by a fast sol–gel process [36] and adapted for 2-photon polymerization process [37]. The hybrid organic-inorganic material exhibits improved transparency, mechanical, and chemical resistance properties compared to standard common organic photoresists. Figure 13 presents microscope images of examples of 3D-printed sol-gel micro-scale optical elements: (a) line shaped phase element, (b) square shaped phase element, (c) rectangular box, (d) cube, (e) pyramid, and (f) dome. The roughness of the elements was measured using a laser scanning confocal microscope (LEXT-5000 Olympus) and was found to be less than 20 nm. The 3D-printed sol-gel based elements were tested for chemical resistance using common solvents such as water, methanol, iso-propanol and acetone. The mechanical stability of the elements was tested using a mechanical profiler with no observed damage. The optical properties were tested for the two phase elements (Figures 13a & 13b). A tailoring lens functionality demonstrated manipulation of an incoming Gaussian beam into line and square intensity-flattened profiles [45]. The use of the hybrid solgel provides tailored material properties, approaching those of glass, meaning better optical quality, higher damage threshold, increased mechanical stability, and vast solvent durability compared to classical organic photoresists used for 3D printing by 2PP process [37]. This opens new and exciting opportunities for compact and robust micro-scale optical devices, by obtaining material properties resembling glass, and overcoming limitation of organic polymers.

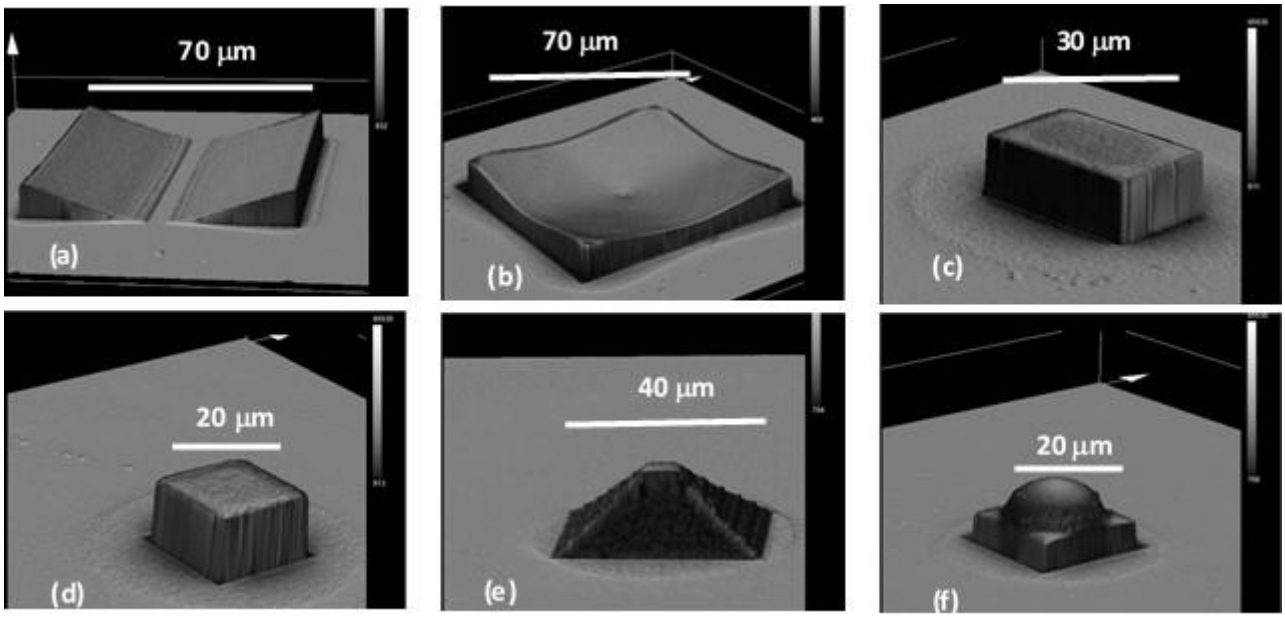


Figure 13: 3D-printed sol-gel based micro-scale optical devices: (a) line shaped phase element, (b) square shaped phase element, (c) rectangular box, (d) cube, (e) pyramid, and (f) dome.

Recently we demonstrated 3D-printing of more complex optical devices, a fiber combiner, based on the 2PP FSG photoresist [38]. We designed a 3D photonic lantern (PL) for multiplexing six single mode (SM) inputs to a similar-sized few-mode fiber at 1.55 micron wavelength. Because of the high index contrast waveguides (Δn~0.44), the 6-mode waveguide has a diameter of 2.1 μm and the SM waveguide has a diameter of 1μm. The PL in this work is intended for interfacing 6-single mode sources with mode field diameters of 6 μm and 35 μm pitch. As a result, mode matching from the source to the PL is required. The Input waveguides are not reaching an SM diameter (1 μm) to make the PL fabrication feasible and mechanically stable. Instead, they begin with an 8.4 μm diameter for efficient coupling to the source and gradually reduce to a 6-mode size (2.1 μm) over a length of 250 μm. For an operation wavelength of 1.55 μm, simulation results show an insertion loss (IL) of 93% (-0.31dB) and a mode dependent loss (MDL) of 97% (-0.13dB). Material loss is -0.15 dB for a device length of 250 μm and can be reduced by modifying the FSG organic content or working in a shorter wavelength spectral range (500 μm-1100 μm). Figure 14a depicts the PL's simulated coupling matrix, while Figure 14b depicts simulated demultiplexing for various modes. As a preliminary fabrication, Figure 14c depicts a SEM image of a 3D structure of a photonic lantern with a 5 μm diameter core size. The structure is printed on a glass slide and is intended to be printed on top of a 6 mode fiber for additional optical characterization.

(a) (b) (c)

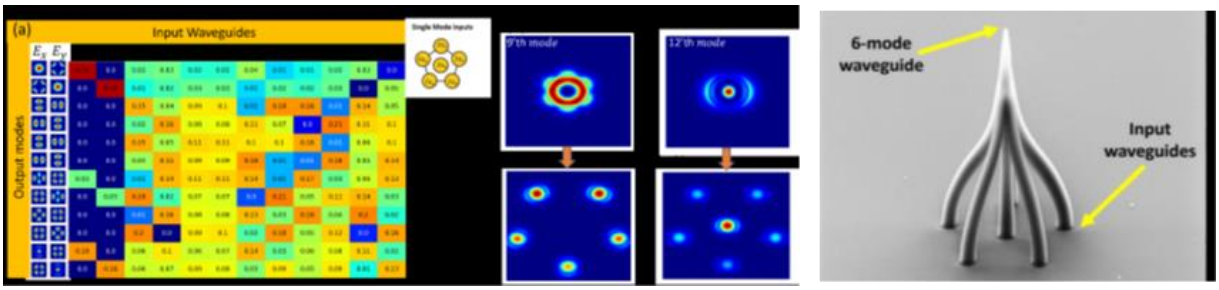


Figure 14: Fiber combiner (a) PL's simulated coupling matrix. (b) Simulated demultiplexing for various modes. (c) a SEM image of a 3D structure 2PP-FSG photonic lantern.

Currently we are checking the ability to print the nonlinear optical filters using hybrid inorganic-organic sol-gel ink doped with appropriate 2PA chromophore. Until now we did not succeed to find the appropriate conditions in which the 2PA chromophore, Fluorene-AF240-$OC_2$ dye, will not be quenched due to photo-degradation during the UV-curing process.

## 4. Conclusions

We studied the use of asymmetric Fluorene-derivative, diphenylamine-fluorene-benzothiazole dye with the geometry of D-π-A, called Fluorene-$OC_2$ or AF240, doped in hybrid sol-gel material as a solid nonlinear optical filter. Due to the fact that Fluorene-$OC_2$ is an asymmetric molecule it is sensitive to the environment. The Fluorene-$OC_2$ was incorporated in a silica based hybrid sol-gel material. Two approaches for the doping procedure were used: “a” adding the dye to the precursor's solution, before hydrolysis; and "b" adding the dye to the final resin, after hydrolysis before polymerization. In the case of "a", an orange sol-gel filter was obtained, while in the case of doping by option "b", a green sol-gel filter was obtained. The two composite materials differs by their optical properties. Specifically, the fluorescence peaks of the two species differ in position and intensity. The absorption peak in both cases is at 400nm, where the fluorescence peak of Fluorene-$OC_2$ green form is at 470nm, resulting in Stokes shift of 3770 $cm^{-1}$, while the fluorescence peak of Fluorene-$OC_2$ orange form is at 670nm, resulting in significantly higher Stokes shift of 8330 $cm^{-1}$. In order to understand these differences we compared the dye performance in sol-gel to the performance in two solutions; toluene, a non-polar solvent and acidic toluene a polar solvent. The obtained results were Stokes shift of 3400 $cm^{-1}$ in toluene solution, with a significantly higher Stokes shift of 8970 $cm^{-1}$ in acidic toluene solution. According to these results we suggested that in case of acidic polar environment a protonated form of the Fluorene-$OC_2$ dye is stable. Moreover, we suggested that a solvatochromic dye can be used to probe the microenvironment in a solid matrix. In this case two segments were found in the hybrid sol-gel. The first segment is obtained when the Fluorene-$OC_2$ dye is doped by option "a", added to the precursor's solution before hydrolysis. In this case, the solvatochromic dye exhibits an acidic polar environment, therefore we can assume the dye is caged inside the sol-gel sols. The second segment is obtained when the Fluorene-$OC_2$ dye is doped by option "b", added to the sol solution after hydrolysis. In this case, the solvatochromic dye exhibit a more non-polar environment, therefore we can assume the dye is caged between the hybrid sol-gel chains and attached to the methyl tails. In addition, by performing femtosecond transition absorption (fsTA) measurements of the Fluorene-$OC_2$ dye orange form, it was demonstrated that intramolecular charge-transfer (ICT) transitions exist which allow several excited-state absorption (ESA) transitions. The existence of ESA transitions suggests that the orange form of Fluorene-$OC_2$ dye is a good candidate for nonlinear optics absorption performance.

In addition, we developed a hybrid organic-inorganic glassy ink based on fast sol-gel process appropriate for 3D-printing with 2-photon polymerization mechanism. We demonstrate 3D-printing of micro-scale optical devices with improved properties. Currently we are checking the ability to print the nonlinear optical filters using hybrid inorganic-organic sol-gel ink doped with appropriate 2PA chromophore.

## 5. References


1. J.M. Hales, D.J. Hagan, E.W. Van Styrland, K.J. Schafer, A.R. Morales, K.D. Belfield, P. Pacher, O. Kwon, E. Zojer, L. Bredas, *J. Chem. Phys*., *121*, 3152, **2004**.
2. D.B. Kevin, J.H. David, W.V.S. Eric, J.S. Katherine, A.N. Raluca, Org. Lett. 1 (**1999**) 1575.
3. D.B. Kevin, J.S. Katherine, M. Wael, A.R. Bruce, *J. Org. Chem*. 65 (**2000**) 4475.
4. K.D. Belfield, A.R. Morales, B.-S. Kang, J.M. Hales, D.J. Hagan, E. W. Van Stryland, V.M. Chapela, J. Percino, *Chem. Mater.* **16**, 4634, **2004**.
5. S. Yao, K.D. Belfield, "Synthesis of Two-Photon Absorbing Unsymmetrical Branched Chromophores through Direct Tris(bromomethylation) of Fluorene", *J. Org. Chem.*, **2005**, 70, 13, 5126.
6. Gvishi, R. , Tank, H., McMillian, Hagan, D.J., Van Stryland, E.W., Katherine, J., Schafer, Yao, S., Belfield, K.D., "Nonlinear absorption and refraction measurements of Fluorene-based molecules via Picosecond Z-scans", (Conference Paper) *SPIE* 5934, 59340C, 1-8 (**2005**).
7. Shivani, Akriti Mishra, Paramjit Kaur, Kamaljit Singh, "Pertual extension of conjugation of fluorine-based donor-acceptor dyads yield diminished nonlinear optical response", *J. Phys. Chem. C*, 127, 1260 (**2023**).
8. M. Wang, V. Nalla, S. Jeon, V. Mamidala, W. Ji, L.S. Tan, T. Cooper, L.Y. Chiang, "Large femtosecond two-photon absorption cross sections of fullersome vesicle nanostructures derived from highly photoresponsive amphiphilic C60-light-harvesting fluorine dyad", *J. Phys. Chem. C*, 115, 18552 (**2011**).
9. X. Lin, D. Tang, T. He, Z. Xu, H. Qiu, Q. Zhang, S. Yin, "A series of novel BODIPI-fluorene copolymers: synthesis, characterization, optical-electronic and nonlinear optical properties", *Spectrochimica Acta Part A: Molecular and Biomolecular Spectroscopy*, 217, 164 (**2017**).
10. G. Ramos-Ortiz, J.L. Maldonado, M.C.G. Hernandez, S. Fomine, N. Frohlich, U. Scerf, F. Galberct, E. Preis, M. Salmon, J. Cardenas, M.I. Chavez, "Synthesis, characterization and third-order optical properties of novel fluorine monomers and their cross-conjugated polymers", *Polymer*, 51, 2351 (2010).
11. R. Gvishi, L.A. Padilha, J. Fu, T.H. McMillian, D.J. Hagan, E.W. Van Stryland, S. Yao and K.D. Belfield, "Nonlinear absorption and refraction process of Fluorene-based molecules via picosecond and femtosecond measurements", *SPIE* 6192 61923C (**2006**).
12. Feng Xu, Zhenwei Wang, Qihuang Gong, "Synthesis, characterization, and optical properties of two-photon-absorbing octupolar molecule with an s-triazine core", *Optical Materials* 29 (**2007**) 723–727.
13. Laura Bekere, Vladimir Lokshin, Mark Sigalov, Raz Gvishi, Peng Zhao, David J. Hagan, Eric W. Van Stryland and Vladimir Khodorkovsky, "Chromenes involving a two-photon absorbing moiety: photochromism via intramolecular resonance energy transfer", *New Journal of Chemistry*, 40 (2), 1143-1148, (**2016**).
14. J.E. Rogers, J. E. Slagle, D.G. MclLean, R.L. Sutherland, M.C. Brant, J. Heinrichs, R. Jakubiak, R. Kannan, L.S. Tan, P.A. Fleitz, "Insight into nonlinear absorbance of two related series of two-photon absorbing chromophores", *J. Phys. Chem* A **2007** 111, 1899.
15. David J. Stewart, Matthew J. Dalton, Rachel N. Swiger, Jennifer L. Fore, Mark A. Walker,Thomas M. Cooper, Joy E. Haley, and Loon-Seng Tan, "Symmetry- and Solvent-Dependent Photophysics of Fluorenes Containing Donor and Acceptor Groups, *J. Phys. Chem*. A **2014**, 118, 5228−5237.
16. R. Gvishi, U. Narang, P. N. Prasad and F. V. Bright, "Probing the microenvironment of polymer-impregnated composite glass using solvatochromic dye". *Chemistry of Materials*, 7 (9) 1703-1708 (**1995**).
17. C. F. Zhao, R. Gvishi, U. Narang, G. Ruland, and P. N. Prasad, "Structures, spectra and lasing properties of new hemicyanine laser dyes". *J. Phys. Chem*., 100 (11) 4526-4532 (**1996**).
18. Brinker CJ, Scherer GW (**1990**) *Sol-gel science*: the physics and chemistry of sol-gel process. Academic press, Boston USA.
19. M. Zdoncyk, B. Potaniec, M. Fiedot-Tobola, T. Baraniecki, J. Cybinska, "Concentration-dependent emission of annealed sol-gel layers incorporated with rhodamine 19 and 6G as the route to tunable high-temperature luminescent materials", *Gels*, 8, 408, (**2022**).

20. R. Mallavia, M.J. Martinez-Tome, R. Vazquez-Guillo, Z. Kahveci, A. Estepa, C. Reyes Mateo," Stabilization of netral polyfluorene in aqueous solution through their interaction with phospholipids and sol-gel encapsulation", *Applied materials & interfaces*, 5, 2952, (**2013**).
21. S. David, D. Chateau, H.J. Chang, L.H. Karlson, M.V. Bondar, C. Lopes, B. Le Guennic, D. Jacquemin, G. Berginc, O. Maury, S. Parola, "High-performance optical power limiting filters at telecommunication wavelengths: when aza-BODIPY dyes bond to sol-gel matrials", *J. Phys. Chem. C*, 124, 24344 (**2020**).
22. D. Chateau, F. Chaput, C. Lopes, M. Lindgren, C. Brannlund, J. Ohgren, N. Djourelov, P. Nedelec, C. Desroches, B. Eliasson, T. Kindahl, F. Lerouge, C. Andraud, S. Parola, "Silica hybrid sol-gel materials with unusually high concentration of Pt-organic molecular guests: studies of luminescence and nonlinear absorption of light", *App. Mater. Interfaces*, 4, 2369, (**2012**).
23. I.C. Vasilliu, I. Ionita, A. Matei, M. Elisa, R. Iordanescu, I. Feraru, A. Emandi, " Homogenous smooth sol gel films doped with organic compounds for nonlinear optics", *Thin Solid Films*, 601, 73, (**2016**).
24. S. Islam, M. Abdullah, "Structural and 3rd order nonlinear optical properties of organic dyes immobilized silica nano-composite", *Optical Materials* 106, 110034, (**2020**).
25. V. Chernyak, R. Reisfeld, R. Gvishi and D. Venezky, "Oxazine-170 in sol-gel glass and PMMA films as a reversible optical waveguide sensor for ammonia and acids". *Sensor and Materials* 2 117 (**1990**).
26. R. Reisfeld, R. Gvishi and Z. Burshtein, "Photostability of the laser action of the Red Perylimide Dye in composite glass". *Journal of Sol-Gel Science and Technology*, 4 (1) 49-55 (**1995**).
27. R. Gvishi, G. S. He, P. N. Prasad, U. Narang, M. Li, F. V. Bright, B. A. Reinhardt and A. G. Dillard, "Spectroscopic studies of new blue laser dyes in THF solution and in composite glass". *Appl. Spect.* 49 834 (**1995**).
28. R. Gvishi, G. Ruland, and P. N. Prasad, "New laser medium: dye-doped sol-gel fiber". *Optics Commun*.,126 (1-3) 66-72 (**1996**).
29. G. S. He, R. Gvishi, P. N. Prasad and B. A. Reinhardt. "Two-photon absorption based optical limiting and stabilization in organic molecule-doped solid materials". Optics Commun., 117 (1-2) 133-136 (**1995**).
30. R. Gvishi, P. N. Prasad, B. A. Reinhardt and J. C. Bhatt, "Third-order optical nonlinear studies of heptamers-doped sol-gel processed silica : polymer composite by degenerate four-wave mixing and optical Kerr gate measurements". *Journal of Sol-Gel Science and Technology*, 9 (2), 157-167 (**1997**).
31. Raz Gvishi, Peng Zhao, Honghua Hu, Galit Strum, Amir Tal, Shmuel Grinvald, Galit Bar, Laura Bekere, Vladimir Lokshin, Vladimir Khodorkovsky, Mark Sigalov, David Hagan, Eric Van Stryland, "Nonlinear solid-state filter based on photochromism induced by 2-photon absorption in a dye-doped sol-gel", SPIE vol. 9181, 9181OJ, (**2014**).
32. R. Gvishi, G. Ruland, and P. N. Prasad, "The influence of structure and environment on spectroscopic and lasing properties of dye-doped glasses", *Optical Material*, 8 (1-2) 43-54 (**1997**).
33. R. Gvishi, "Fast Sol-Gel Technology - from fabrication to Applications", *Journal of Sol-Gel Science and Technology*, 50 (2) 241-253 (**2009**).
34. R. Gvishi, G. Strum, A. Englander, "UV-curable glassy material for the manufacture of bulk and nano-structured elements", *J. Europ. Opt. Soc. Rap. Public*. 7, 12002 (**2012**).
35. Tamara Hanuhov, Eric Asolin, Raz Gvishi, "Evaluation of opto-mechanical properties of UV-cured and thermally-cured sol-gel hybrids monoliths as a function of organic content and curing process", *Journal of non-Crystalline Solids* 471, 301-311 (**2017**).
36. Raz Gvishi and Ilan Sokolov, "3D Sol-Gel printing & Sol-Gel bonding for fabrication of Macro- and Micro/Nano-structured photonic devices", *Journal of Sol-Gel Science and Technology*, 95, 635–648 (**2020**).
37. Shlomi Lightman*, Moran Bin-Nun*, Galit Bar, Gilad Hurvitz, Raz Gvishi, "Structuring light using sol-gel hybrid 3D-printed optics prepared by two-photon polymerization", *Applied Optics*, 61, 1434, (**2022**).
38. M. Bin Nun, G. Bar, Y. Dana, D. M. Marom, S. Lightman and R. Gvishi, "Microscale Sol-Gel Optical Devices Printed by Two-Photon Polymerization and Direct Laser Writing", Oral presentation at *CLEO* San Jose, California, USA, May **2023**.
39. Rogers JE, Slagle JE, Krein DM, Burke AR, Hall BC, Fratini A, McLean DG, Fleitz PA, Cooper TM, Drobizhev M, Makarov NS, Rebane A, Kim K-Y, Farley R, Schanze KS, "Platinum acetylide two-photon chromophores". *Inorg Chem* 46: 6483–6494 (**2007**).

40. Reban A, Drobizhev M, Makrov NS, Wicks G, Wunk P, Steaneko Y, Haley JE, Krein DM, Fore LJ, Burke AR, Slage JE, McLean DG, Cooper TM, “Symmetry breaking in platinum acetylide chromophores studied by femtosecond two-photon absorption spectroscopy”. *J Phys Chem A* 118:3749–3759 (**2014**)
41. Chateau D, Liotta A, Lunden H, Lerouge F, Chaput F, Krein DM, Cooper TM, Lopes C, El-Amay AAG, Lindgren M, Parola S, “Long distance enhancement of nonlinear optical properties using low concentration of plasmonic nanostrctures in dye doped monolithic Sol-Gel materials”. *Adv Func Mater*. https://doi.org/10. 1002/adfm.201601646 (**2016**).
42. Cooper TM, Haley JE, Krein DM, Burke AR, Slagle JE, Mikhailov A, Reban A, “Two-photon spectroscopy of a series of platinum acetylide chromophores: conformation-induced ground-state symmetry breaking”. *J Phys Chem* A 121:5442–5449 (**2017**).
43. Shlomi Lightman, Raz Gvishi, Gilad Hurvitz, and Ady Arie, "Shaping of light beams by 3D direct laser writing on facets of nonlinear crystals", *Optics Letters*, 40 (19), 4460-4463 (**2015**).
44. Shlomi Lightman, Raz Gvishi, Gilad Hurvitz, and Ady Arie, “Miniature wide-spectrum multiplexer for vortex beams produced by 3D laser printing”, *Optica* 4(6) 605-610 (**2017**).
45. Shlomi Lightman, Raz Gvishi, Gilad Hurvitz, and Ady Arie, "Tailoring lens functionality by 3D laser printing", *Applied Optics*, 56 (32), 9038-9043 (**2017**).
46. S. Lightman, I. Bleyhman, L. Omer, G. Hurvitz , R. Gvishi, L. A. Rusch, A. Arie, “Integrated orbital angular momentum mode sorters on vortex fibers”, *Optics Letters*, 47, 3491 (**2022**).
47. S. Lightman, O. Porat, R. Gvishi, G. Hurvitz, “Vortex-Bessel beam generation by 3D direct printing of a twisted axicon on a fiber tip”, *Optics Letters*, 47, 5248 (**2022**).
48. R. Kannan, L Tan, "Two-photon absorbing chromophores containing polymerizable olefinic groups", *US Patent* US7067674B1, **2006**.
49. Mariana Pokrass, Irina Gouzman, Galit Bar, Raz Gvishi, "Infrared and X-ray photoelectron spectroscopy studies of hybrid organic/inorganic fast sol–gel glasses", *Optical Materials* 34 (2) 341–346 (**2011**).

**List of Publications and Significant Collaborations that resulted from your AOARD supported project:**

In standard format showing authors, title, journal, issue, pages, and date, for each category list the following:

a) papers published in peer-reviewed journals,
b) papers published in peer-reviewed conference proceedings,
c) papers published in non-peer-reviewed journals and conference proceedings,
d) conference presentations without papers,
e) manuscripts submitted but not yet published, and
f) provide a list any interactions with industry or with Air Force Research Laboratory scientists or significant collaborations that resulted from this work.

Manuscripts before submission:

1. Ramamurthi Kannan, Zhenning Yu, Lauren M. Loftus, Loon-Seng Tan, Tod A. Grusenmeyer, Ayelet Teitelboim, Galit Bar, Raz Gvishi, "Controlling optical properties depending on formulation in nonlinear optical solid filters based on hybrid sol-gel glasses containing asymmetric fluorene-derivative dyes", will be submitted soon.

Papers published in peer-reviewed journals:

2. Shlomi Lightman*, Moran Bin-Nun*, Galit Bar, Gilad Hurvitz, Raz Gvishi, "Structuring light using sol-gel hybrid 3D-printed optics prepared by two-photon polymerization", *Applied Optics*, 61, 1434, (**2022**).

Papers published in peer-reviewed conference proceedings:

3. M. Bin Nun, G. Bar, Y. Dana, D. M. Marom, S. Lightman and R. Gvishi, "Microscale Sol-Gel Optical Devices Printed by Two-Photon Polymerization and Direct Laser Writing", Oral presentation at *CLEO* San Jose, California, USA, May **2023**.

Conference presentations without papers:

4. Moran Bin-Nun, Shlomi Lightman, Galit Bar, Nurit Atar , Gilad Hurvitz, Raz Gvishi, "3D-printed sol-gel micro-scale optical devices by Direct Laser Writing (DLW) via 2-Photon Polymerization (2PP) Process", Oral presentation at ICMAT-MRS 2023, Singapore, May **2023**.

The work is a collaboration with Air Force Research Laboratory scientists:
Ramamurthi Kannan, Zhenning Yu, Lauren M. Loftus, Loon-Seng Tan, Tod A. Grusenmeyer.

**Attachments:** The above Publications are attached.

**Additional documents attached:**

1. DD882 REPORT OF INVENTIONS.
2. FEDERAL FINANCIAL REPORT